Available online at www.sciencedirect.com

ScienceDirect

Composite Structures 84 (2008) 271–281

COMPOSITE STRUCTURES

www.elsevier.com/locate/compstruct

Blast resistance of polyurea based layered composite materials

Srinivasan Arjun Tekalur [a], Arun Shukla [a,*], Kunigal Shivakumar [b]

[a] Dynamic Photomechanics Laboratory, Department of Mechanical Engineering and Applied Mechanics, University of Rhode Island, 206 Wales Hall, 92 Upper College Road, Kingston, RI 02881, USA

[b] Center for Composite Materials Research, Department of Mechanical and Chemical Engineering, North Carolina A&T State University, Greensboro, NC, USA

Available online 2 September 2007

Abstract

Composite materials have been used in applications involving blast and ballistic impacts, and are considered effective materials in absorbing the energy of blast. Application of polyurea to composites, as a shock mitigation material is a relatively new idea. In this study, layered and sandwich composite materials, comprising of polyurea (PU) and E-glass vinyl ester (EVE) composite are experimentally evaluated for effective blast resistance using a shock tube. Rectangular plates of the plain–woven composite and the layered composite, simply supported along two edges and free along the other two were subjected to controlled blast. The free end of the plate was observed real time using a high-speed camera during the dynamic bending due to the blast. Results indicate that addition of the polyurea layer on the impact face considerably increases the blast resistance. Further, sandwich materials prepared by sandwiching the polyurea between two composite skins had the best blast resistance compared to the layered and the composite plates.

Keywords: Glass fiber composites; Polyurea; Layered and sandwich construction; Blast resistance; Structural response

1. Introduction

Composite materials have widespread applications in naval and defense structures. With the advent of innumerous blast attacks on these structures during service and during regular warfare exercises, proper understanding of blast response and resistance is essential to design and develop new materials and methods to enhance the same. Response of monolithic plates [1,2] and conventional sandwich structures [3] to blast loading has been studied. There also exist studies on homogeneous materials subjected to transient loadings [4–8]. But, experimental observations on the real time response of composite and layered structures under blast are limited. In recent times, researchers have proposed polymer-based coatings on buildings and structures to enhance blast resistance [9]. In addition to energy absorption, various studies have directed interest towards reducing the amount of material required to resist blast loading on the structure. Spraying or application of polyurea over conventional composite structures is one such approach. The addition of polyurea to the composite structures introduces complexity to the structural response due to several factors including the nonlinear material behavior and dispersive wave propagation in polyurea. The rate sensitive behavior of polyurea has been an interest of study [10–12] and has been shown that material behavior of polyurea is dependent on the constitution, loading rate and temperature. In their previous work, the authors characterized the blast resistance of plain–woven composites under different boundary conditions [13,14]. In the present study, the dynamic response of layered materials and blast resistance of structural elements fabricated by applying polyurea over conventional composites is studied. The dynamic characterization was performed using a split Hopkinson pressure bar and the blast response was studied using a shock tube. In addition to these layered materials, sandwich materials were also fabricated and their blast resistance was evaluated experimentally.

* Corresponding author. Tel.: +1 401 874 2283.
E-mail address: shuklaa@egr.uri.edu (A. Shukla).

0263-8223/$ - see front matter © 2007 Elsevier Ltd. All rights reserved.
doi:10.1016/j.compstruct.2007.08.008

2. Materials

2.1. E-glass vinyl ester composite (plain–woven composite)

The resin system used was Dow Chemical's Derakane 510A-40. The glass fabric chosen was woven roving E-glass supplied by Fiber Glass Industries' (FGI). The areal weight was 610 g/m^2 (18 oz/sqyd) with an unbalanced construction having 59% and 41% of fibers in warp and fill directions respectively. Further details about the composite material can be found in [15].

2.2. Polyurea

Polyurea is a cross-linked amorphous isocyanate monomer or prepolymer and polyamine curative. To be classified as a polyurea, the compound must contain at least 80% polyamine.

There are two basic types of polyurea: aromatic and aliphatic. An aromatic type, EP JS provided by Engineered Polymers International, was used in this research. Polyureas typically have 100% solids, low-out gassing, low shrinkage resistant to moisture, and adhere well with many substrates (concrete, plastic, and steel). Glass transition temperature for cured systems can range from −60 °F to 480 °F. Polyurea is extremely resistant to thermal shock and blast effects. It is also self-extinguishing when flame is removed from surface. The EP JS has 20.34 MPa (2950 psi) tensile strength, 350% elongation, 11.16 MPa (1620 psi) modulus, and 87.5 kN/m (500 lb/in) tear strength.

2.3. Polyurea layered sandwich composite panel fabrication – VARTM panels

The VARTM-fabricated panels were produced from a plain weave E-glass fabric type, Rovcloth FGI-1854 provided by Fiber Glass Industries. Fabric lay-up was a 14-ply balanced/symmetric for a nominal vacuum-debulked thickness of 6.35 mm (0.25″) for nominal 0.965 m × 0.965 m (38″ × 38″) area. The brominated bisphenol-A epoxy vinyl ester resin type, Derakane 510A-40 provided by Ashland Chemical, was catalyzed with CoNap, 2,4-P, and MEKP. The vinyl ester resin was degassed at 736.6 mm Hg (29″ Hg) and vacuum impregnated at 635 mm (25″) Hg into the fabric stack at room temperature. The green-cured panel was removed from the vacuum bag after 6 hours and then post cured. The fiber volume fraction of the panels was 0.605. Details of the process are in Ref. [16,17].

A second panel of a 7-ply balanced/symmetric lay-up in 6.35 mm (0.25″) thickness × 0.965 m (38″) × 0.482 m (19″) nominal area was also fabricated for the composite sandwich configuration. A third set of 4-ply unidirectional panel was fabricated for mechanical characterization. Cured panels were cut to the required sizes with a water-cooled diamond blade tile saw for use as casting substrates for the polyurea coating.

2.3.1. Sandwich panels

Polyurea castings of 6.35 mm (0.25″) and 3.18 mm (0.125″) thick were made as per the instructions of the material supplier. These castings were then bonded to composite panels of required size, as per the plan (one-side, both side, and sandwiched by composite panels). Further details of the specimen sizes are provided in Section 3.2.

2.4. Dynamic characterization (Hopkinson bar experiments)

Dynamic characterization of plain–woven composite, polyurea and layered materials were performed using a Split Hopkinson Pressure Bar (SHPB) setup. A basic schematic of the setup is shown in Fig. 1. Details of the SHPB experimental procedure and data analysis can be found in the literature [18,19]. The bar diameter of the SHPB setup used in these experiments was 0.05 m (2″) and the specimen diameter was 0.038 m (1.5″). The thickness of the plain–woven composite and the layered material was 0.005 m (0.2″) and 0.01 m (0.4″) respectively. The layered material was made of 0.005 m (0.2″) each of plain–woven composite and polyurea. Several dynamic experiments were performed on the plain–woven composite, polyurea and layered material with polyurea facing the impact bar as well as plain–woven composite facing the impact bar. Figs. 2 and 3 show the true stress–true strain response obtained for plain–woven composite and polyurea, respectively. The polyurea samples were subjected to strain rates of 800 s^{-1} and the composite samples were subjected to strain rates of 1900 s^{-1}. In case of polyurea, a flow stress of 10 MPa was observed at 1% strain and this level was sustained up to 4% strain. Beyond the 4% strain, a strain hardening effect is observed in these materials, with the stress increasing in an almost linear fashion up to strain levels of 8%. In case of the composites, a peak compressive stress of 350 MPa is observed at 3–4% strain.

The dynamic stress–strain behavior of layered material at strain rates of 1100 s^{-1}, is shown in Fig. 4. When the layered sample was subjected to dynamic compression, the peak compressive stress was not characterized by a single point. The maximum strength observed was lower than the plain composite but higher than the polyurea sample.

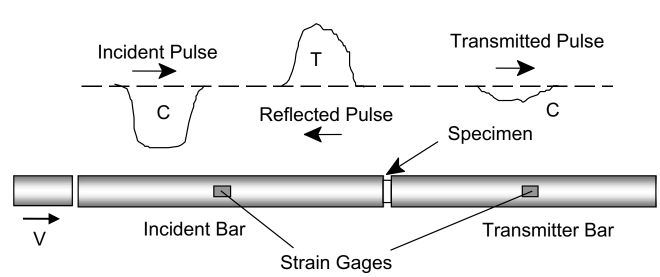

Fig. 1. A Schematic of the Split Hopkinson Pressure Bar (SHPB) setup and typical pulses obtained.

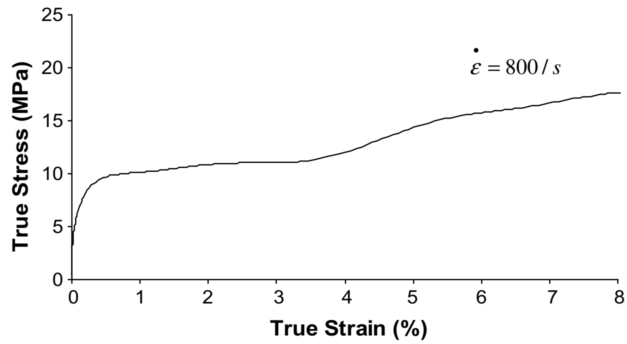

Fig. 2. True stress–strain response of polyurea under dynamic loading conditions.

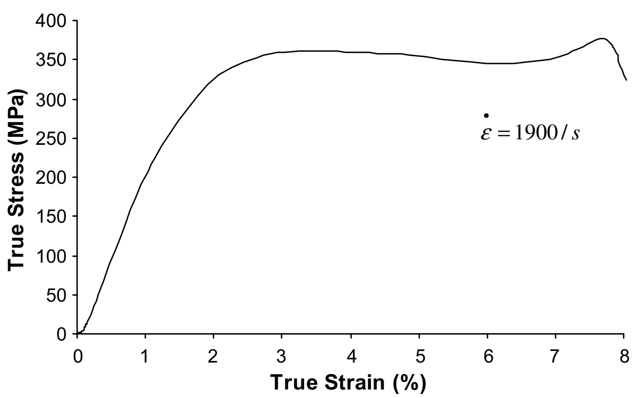

Fig. 3. True stress–strain response of plain–woven composite under high strain rate of loading.

The peaks were observed at strain levels of 1.3–1.5%, 5.3–5.5% and 14.5–14.7%. The maximum strength was observed at the third peak corresponding to 107 and 99 MPa for PU/EVE and EVE/PU respectively. It is observed that direction of impinging the load did not affect the response of the layered material significantly. Whether polyurea was facing the incident bar or transmitter bar, the stress-strain response in both the cases was very close to each other. Although this was true in the SHPB testing, this behavior was not evident in structural applications, as shown later.

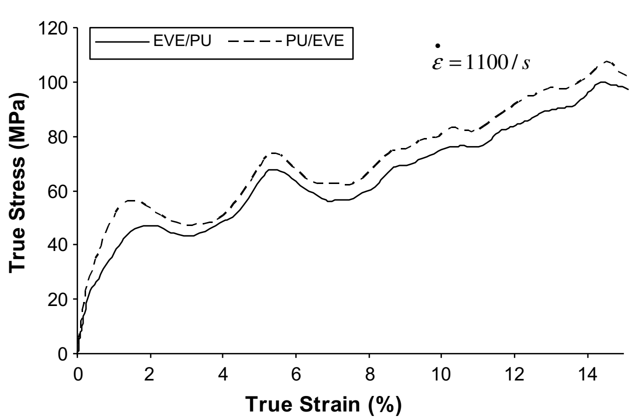

Fig. 4. True stress–strain response of EVE/PU and PU/EVE layered composite under high strain rate of loading.

3. Experimental methodology

The experimental program consisted of subjecting rectangular panels of plain–woven composite, layered and sandwich materials to blast loading of varying intensities and form. Blast loading can be produced by various means. Explosives are widely used to provide rapid loading rates with accompanied pressure loading due to expansion of the gases and products of the explosion. Controlling the rate of explosive loading and obtaining real time data in such explosions are experimental challenges and require adequate safety procedures. A shock tube is a much more controlled method of obtaining similar blast loading effects. Since there is no actual burning of materials involved, it is much cleaner and damage caused in the specimen is confined to pressure applied by the sudden expansion of the gases. The present study utilizes a shock tube for applying blast loading to the composite panels.

3.1. Shock blast loading

In its simplest form a shock tube consists of a long rigid cylinder, divided into a high-pressure driver section and a low pressure driven section, which are separated by a diaphragm. The tube is operated by pressurizing the high-pressure section until the pressure difference across the diaphragm reaches a critical value and it ruptures. This rapid release of gas creates a shock wave, which travels down the tube to impart air blast loading on a specimen.

A photograph of the shock tube facility at the University of Rhode Island is shown in Fig. 5. The shock tube facility in the present study has an overall length of 8 m and is divided into a 1.82 m driver section, 3.65 m driven section and a final 2.53 m muzzle section. The diameter of the driver and driven section are 0.15 m. The final diameter of the muzzle section that is in contact with the specimen is 0.07 m. The driver gas is Helium and the driven gas is ambient air. Mylar diaphragms are ruptured due to pressure differential created between the driver and driven section, which develops and drives a shock wave down the length of the shock tube. A pressure sensor (PCBA23) at the end of the muzzle section measures the impact shock

Fig. 5. The shock tube facility to produce controlled blast loading.

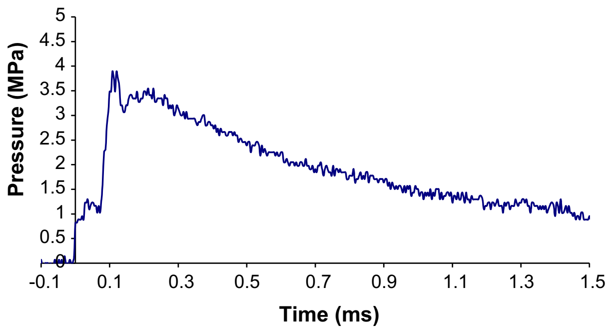

Fig. 6. Typical pressure profile obtained from the shock tube. The input shock and reflected pressures are seen here.

pressure and the reflected pressure during the testing. A typical pressure profile obtained at the sensor location is shown in Fig. 6.

The first peak in the signal is the "input shock pressure" and the second peak is the "reflected pressure". The input shock pressure remains the same for given number of mylar diaphragms while the reflected pressure is dependent on the material on which the shock is impinged upon. Calibration of the shock tube was performed to obtain the input shock pressure for given mylars and can be found in [20]. Table 1 summarizes the values for input and reflected shock pressures obtained for the materials tested in this study. A break circuit with appropriate triggering mechanism and high-speed recording equipments are used for measuring the shock wave velocities.

Table 1
Measured shock and reflected pressures

Material	Input shock pressure (MPa)	Reflected pressure (MPa)
EVE	0.45	1.28
	0.62	1.57
PU/EVE	**0.62**	**1.55**
	0.75	**2.20**
EVE/PU/EVE	0.75	2.01
	1.03	2.20
	1.18	2.93

3.2. Plate geometry and boundary conditions

Rectangular plates of size 0.23 m × 0.102 m (9″ × 4″) were fabricated for the study. The plates were simply supported over a span of 0.152 m (6″) along two edges (shorter edges) and the other two edges were free. The blast loading covered a circular region of 76 mm (3″) diameter, as shown in Fig. 7.

The panels of plain–woven composite were 6 mm (0.25″) nominal thickness and panels of layered composite were 12 mm (0.5″) nominal thickness that includes 6 mm (0.25″) of plain–woven composite and 6 mm (0.25″) of polyurea coating. The layered composites were tested in two different ways, namely,

1. PU side facing the shock blast (henceforth referred as PU/EVE).
2. EVE side facing the shock blast (henceforth referred as EVE/PU).

Two types of sandwich composite structures were studied under blast loading conditions. Whereas one had a soft core (PU) sandwiched between two hard skins (EVE), the other had a hard core (EVE) sandwiched between two soft skins (PU). The sandwich composites along with their dimensions are given below

(1) 3 mm (0.125″) EVE + 6 mm (0.25″) PU + 3 mm (0.125″) EVE (EVE/PU/EVE sandwich),
(2) 3 mm (0.125″) PU + 6 mm (0.25″) EVE + 3 mm (0.125″) PU (PU/EVE/PU sandwich).

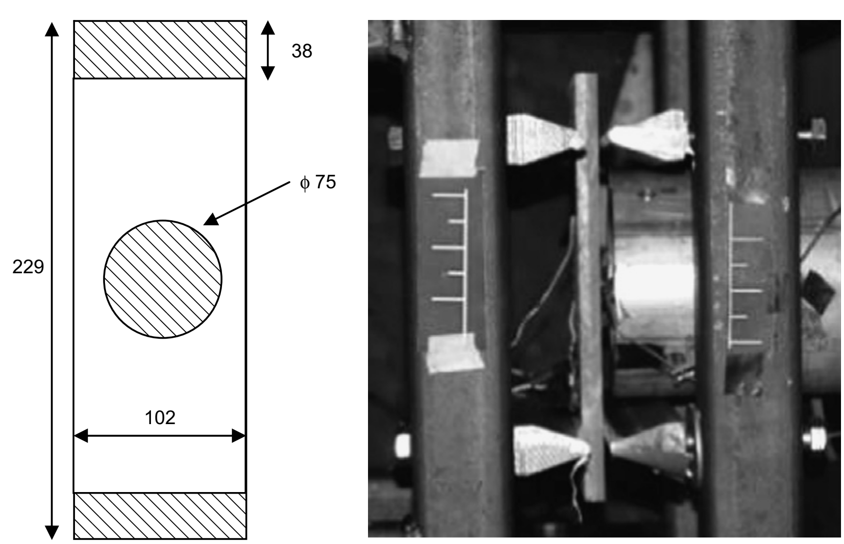

Fig. 7. Sketch of the specimen depicting the loading and boundary areas (all dimensions are in mm). (b) Actual specimen held in simply supported condition at the end of a shock tube.

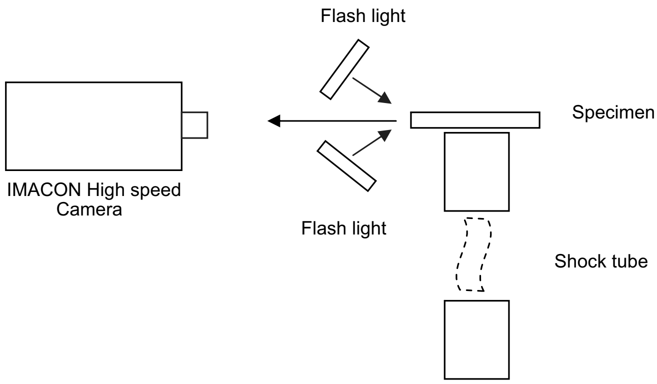

Fig. 8. Schematic of the setup to measure real time deformations in composite plates under blast loadings.

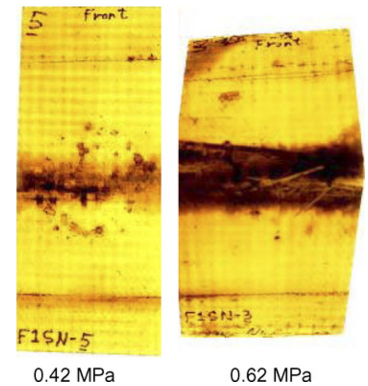

Fig. 9. Damage in E-glass/vinyl ester composite plates under blast loading of varying intensities.

3.3. High-speed digital imaging

Fig. 8 shows the schematic of the setup used for measuring the real time deformation in the plates under blast loading conditions. One of the free ends of the plate is viewed from the side using an IMACON high-speed camera. This camera is capable of taking 16 pictures at framing rates as high as 200 million frames/s with exposure times as low as 5 ns. Typical blast loading events are in the order of 2–6 ms and the deformation of the plate is recorded using the camera over the response period of the plate. Post analysis of these images provided deformation-time history of the center point of the plate during the deformation. Such plots were used as a parameter for comparing the performance of these materials under different blast loading conditions.

4. Results and discussion

4.1. Blast resistance

Blast resistance was characterized using three main parameters, namely macroscopic visual examination, microscopic examination and real time measurements. The macroscopic and microscopic study involved identification of the different damage modes and extent of damage on the panels.

4.1.1. Visual examination

Damage in the EVE panels was concentrated predominantly in the central region as shown in Fig. 9 (photograph taken utilizing a bottom light source). Macroscopic visual damage in the layered and sandwich were also characterized by the extent of damage in the central region (Figs. 10 and 11). A panel is deemed to be "completely failed" when a permanent deformation more than 2.5 times the thickness is produced. This parameter holds true even in the layered and sandwich material systems due to two main factors:

(1) The volume and hence the net weight of the composite is same in all the cases.
(2) The modulus of polyurea is an order of magnitude (5–10 at strain rates of 1000 s^{-1}) less than the modulus of composite.

4.1.1.1. PU/EVE layered material. Whereas panels of plain–woven composite failed at an incident shock pressure of 0.62 MPa, the PU/EVE layered composite required 0.76 MPa of incident shock pressure to fail. Damage progression in PU/EVE layered composite was very similar (Fig. 10) to the damage progression in EVE but the pressure required to induce the same level of damage was higher in case of the layered composite.

4.1.1.2. EVE/PU layered material. In the reverse case (EVE/PU), when EVE was on the strike face, the weaker compressive strength (compared to the tensile strength) of EVE attributed to extensive damages observed in the plate, particularly on the strike face which comprised of glass composite material. The strike face of EVE/PU material had higher delamination area signified as bright white regions in Fig. 20.

4.1.1.3. EVE/PU/EVE sandwich material. The EVE/PU/EVE sandwich composite system showed minimal damage as shown in Fig. 11 under increasing blast loading intensities. These minimal damages in the panels were visualized on the strike face predominantly and there is no evident of external damage on the rear face. On a macroscopic scale, no damage was observed in the EVE/PU/EVE sandwich system despite the fact that these sandwich panels were subjected to 85% higher pressure than the plain–woven composite and 33% higher pressure than the PU/EVE layered material. Fig. 11 also shows the side view of the sandwich panels after being subjected to increasing intensities of blast loadings. There was no visible damage or deformation induced in them due to the blast loads.

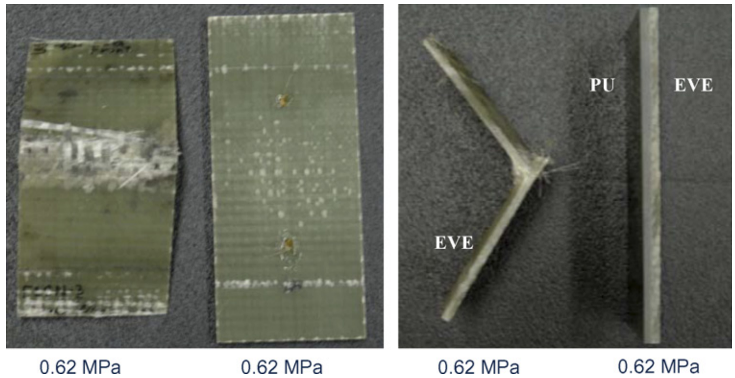

Fig. 10. Damage in E-glass/Vinyl ester composite and layered plates under blast loading of same intensities.

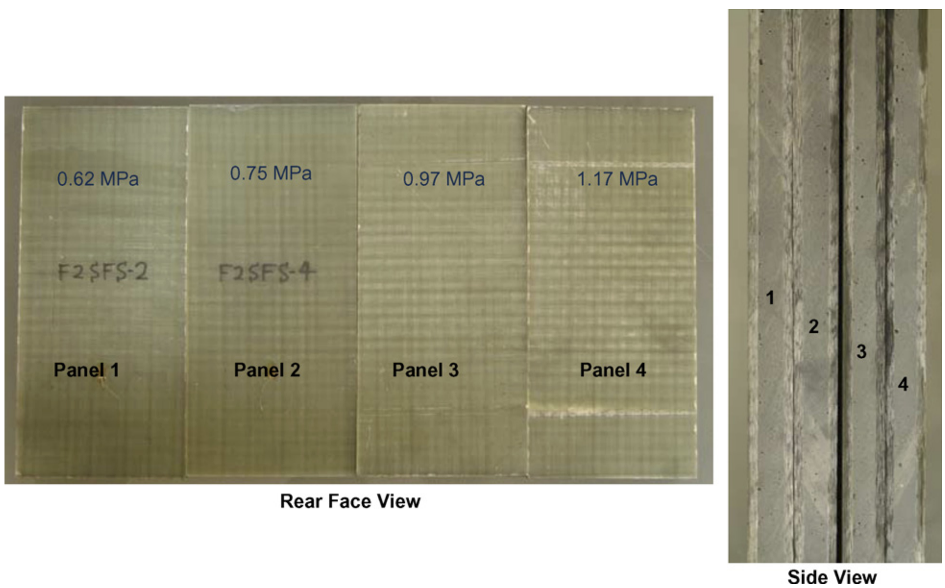

Fig. 11. Four different EVE/PU/EVE sandwich composite plates under blast loading of varying intensities (shock pressure shown in inset).

The damage behavior of soft-core (EVE/PU/EVE) composites was different from that of the hard-core sandwich (PU/EVE/PU). Under similar magnitude of loading (1.17 MPa input pressure), PU/EVE/PU panel showed signs of failure as wrinkles on the strike face and shear failure on the composite core (Fig. 12). Though the hard-core sandwich construction did perform better than the monolithic composite plates, owing to the relatively weaker performance of this configuration when compared to the soft-core, several experiments were performed and attention is focused on the soft-core composites than the hard-core sandwich.

4.1.2. Microscopic examination

Microscopic analysis of undamaged (Fig. 13) and damaged specimen (Figs. 14–16) was done using a Nikon SMZ Microscope. Regions marked as Fiber and Matrix denotes the longitudinal and transverse fiber directions, which also contains the matrix polymer in different proportions.

4.1.2.1. EVE composite. The damage modes observed in blast loaded plain–woven composite included fiber breakage and interface failure. The tensile properties of these composites are superior to the compressive properties. This explains the initiation and the mode of damage on the impact side, which is predominantly under compression. Crushing and cleavage of the longitudinal fiber is observed in these panels, as shown in Fig. 14. The straight cleavage of a longitudinal fiber bundle close to the mid section observed in the figure suggests that the fiber bundle had been crushed compressively during the initial phase of loading and subsequently pulled in tension due to reflection of the waves from the rear surface, leading to an interface failure between the longitudinal and transverse fiber regions.

4.1.2.2. PU/EVE layered material. Addition of a PU layer provides additional modes of damage and hence added energy dissipation mechanisms. In addition to the interface between the transverse and longitudinal fiber directions,

Fig. 12. Side view and strike face view of PU/EVE/PU layered sandwich plates after being subjected to shock blast loading of input pressure 1.17 MPa.

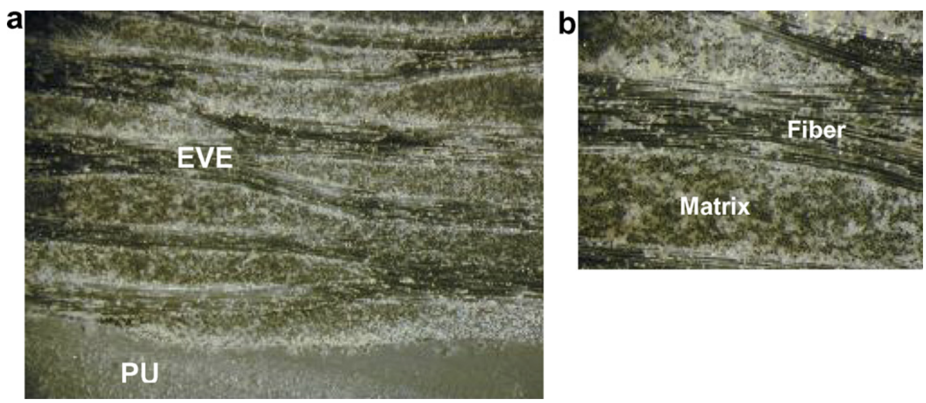

Fig. 13. (a) Microscopic view of an undamaged interface region of PU–EVE in a layered composite. (b) Close view of the fiber–matrix region in the EVE composite.

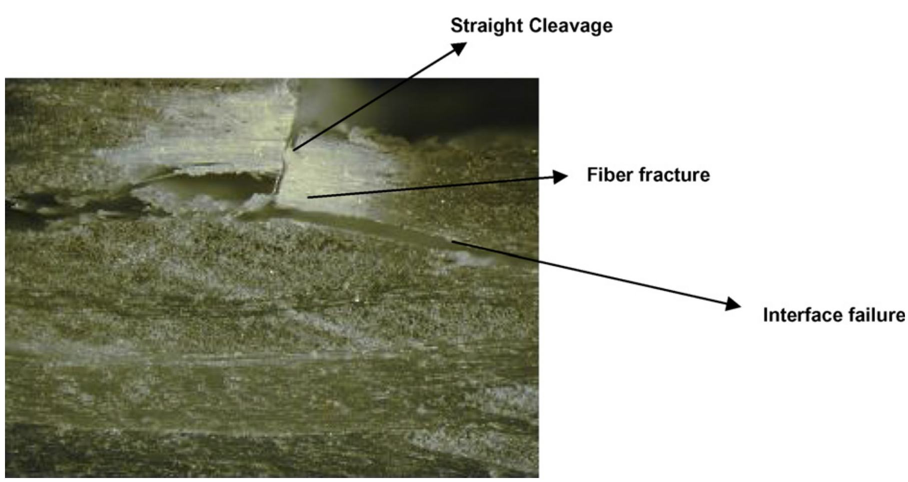

Fig. 14. Microscopic view of damaged region in EVE composite subjected to shock blast pressure of 0.45 MPa. Shown here is the impact side.

the layered materials also have a PU interface with these directions. When studied under the microscope, the predominant damage modes observed in PU/EVE layered materials were

1. Fiber direction tensile failure.
2. Matrix direction failure (observed as voids created through tensile separation).
3. PU-EVE Interface failure (with both the directions).

As noted, the damage modes observed in PU/EVE was predominantly tensile failure patterns. It is also observed that the bonding between Polyurea and transverse layer is weaker than the bonding between Polyurea and longitudinal fiber directions when a layered composite plate is subjected to blast.

4.1.2.3. EVE/PU layered material. When the loading direction was reversed (i.e., EVE on the impact side), compres-

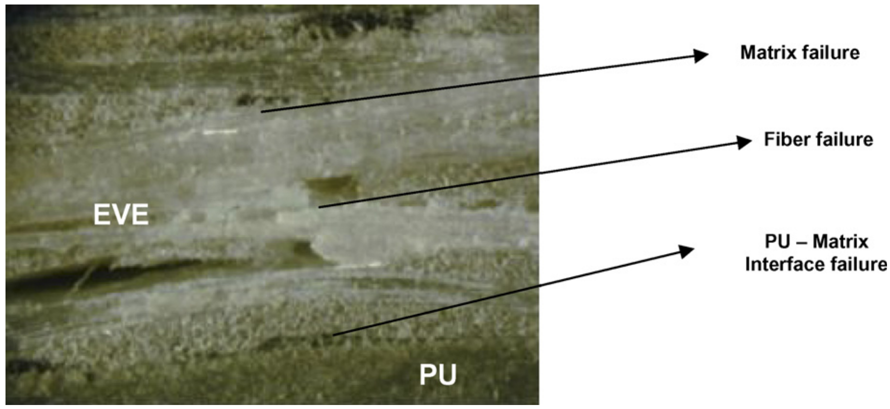

Fig. 15. Microscopic view of damaged region in PU/EVE layered composite subjected to shock blast pressure of 0.62 MPa. Shock blast impact was on the PU side.

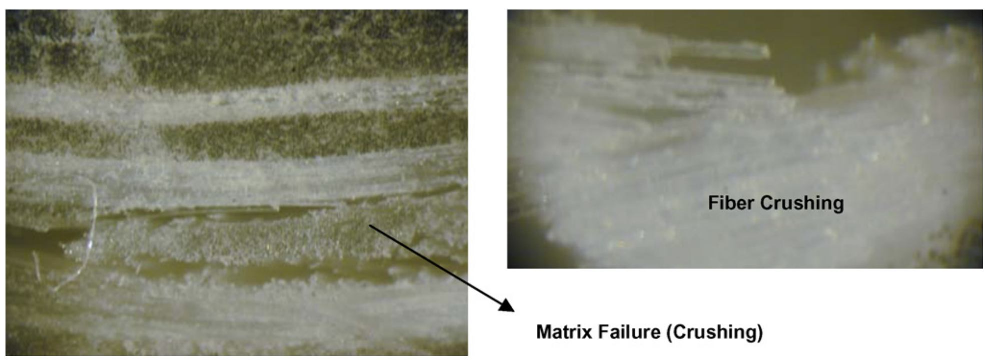

Fig. 16. Microscopic view of damaged region in EVE/PU layered composite subjected to shock blast pressure of 0.75 MPa. Shock blast impact was on the EVE side.

sion dominated failure mode (fiber crushing) was observed (Fig. 16). Again, the interface between polyurea and the transverse fiber direction was observed to be weaker than the interface between polyurea and longitudinal direction. In these layered materials, the microscopic failure mode was dominated by compressive failure patterns like crushing of the transverse and longitudinal fibers. The macroscopic failure patterns also correspond to compressive and shear failure on the strike face of composite plates.

The strengthening or the enhanced blast performance in the layered composite can be attributed to factors like

1. Energy dissipation due to the nonlinear and highly rate dependent properties of the polyurea layer.
2. Energy dissipation in the failure of polyurea-composite interfaces.

But the explanation for observance of better performance of a specific orientation (PU/EVE) needs a thorough understanding. It was already observed in the Hopkinson bar experiments that when the loading is uni-axial, the stress response is not significantly different whether the polyurea faces the impact or composite faces the impact. But, in case of blast loading of a layered plate, wherein the loading induces multi-dimensional stress fields, an additional strengthening mechanism is involved. When polyurea is on the strike face, the composite lamina that is in direct contact with the polyurea is provided with strengthening against compressive and shear failure. So the damage initiation in this lamina will require additional energy from the blast. This will not be true when the composite lamina faces the initial blast directly. The impact face, wherein the first lamina is exposed to a severe compressive zone, begins to fail and hence, the overall strength of the structure reduces progressively as the blast loading progresses. Since the reinforcement of polyurea was on the tensile zone and not the compressive zone, the enhancement in blast performance of these layered composites were comparitatively lower than when the polyurea faced the blast loading.

These conclusions were further evidenced in the macroscopic visual of the composite side in layered composites (Fig. 20) and the observed microscopic failure modes (Figs. 15 and 16).

4.2. Real time measurements

High-speed digital imaging provided real time deflection of the composite, layered and sandwich plates subjected to blast loadings. Typical inter-frame time in

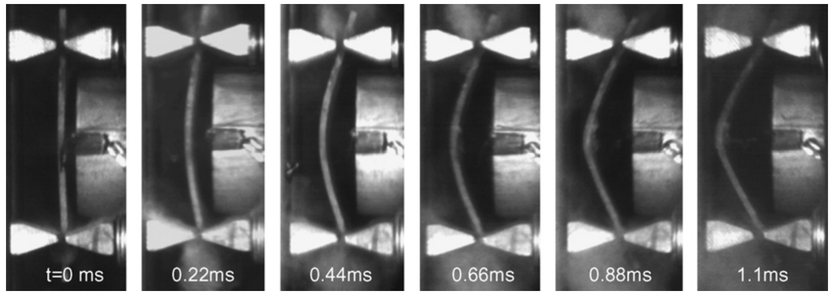

Fig. 17. Typical real-time deformation event of a plain–woven composite plate, when subjected to blast load (0.60 MPa).

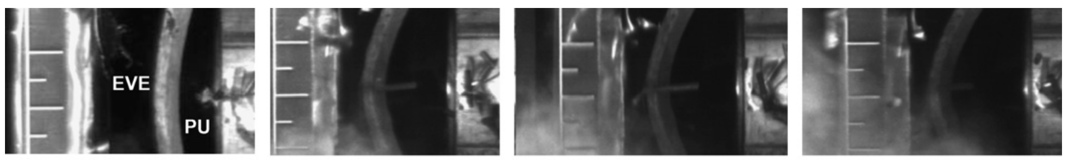

Fig. 18. Typical real-time deformation event of a polyurea/EVE layered composite plate, when subjected to blast load (0.75 MPa) EVE.

these photographs is in the order of 100–250 microseconds and exposures varied from 500–1000 ns. Figs. 17–19 show the real time deflection in plain–woven composite, EVE/PU and PU/EVE materials. Whereas the plain–woven composite failed at an incident pressure of 0.6 MPa, the EVE/PU failed at 0.76 MPa and the PU/EVE sustained considerable visual damage but did not fail completely.

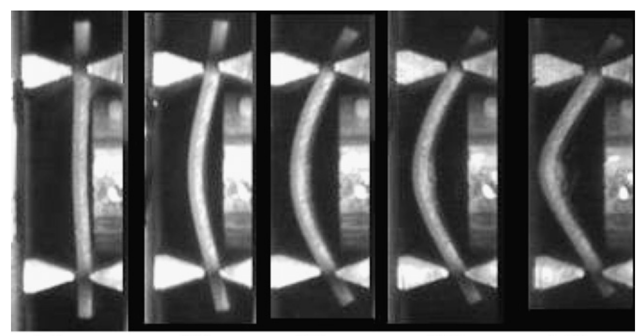

Fig. 19. Typical real-time deformation event of a EVE/PU layered composite plate, when subjected to blast load (0.75 MPa).

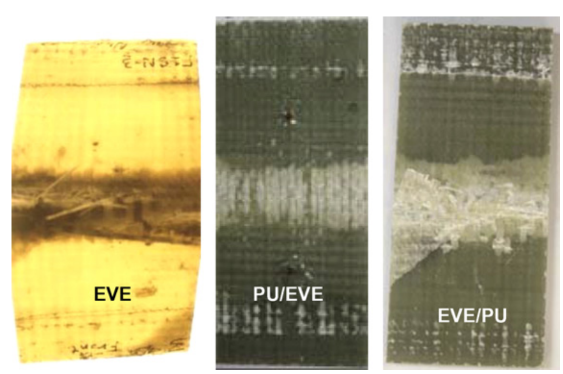

Fig. 20. Post blast view of the plates shown in Figs. 17–19. The EVE composite side is shown in the layered materials.

4.2.1. Center point deflections

The deflection of center point of the plate was calculated from the high-speed images. Figs. 21–23 show the deflection time history of the plain–woven composite, layered and sandwich composite materials. The input pressure is quoted on the legend for each material. These plots reveal that the deflections observed in the layered and sandwich construction was lower than those observed in the plain composite plates, as expected. The quantitative estimate of reduction in deflections can be observed from these plots. Also to be noted is that the input blast pressure is much lower for the plain composite compared to the layered and sandwich constructions.

Fig. 24a and b provides a normalized plot of deflections per unit thickness of the plain composite, layered and sandwich materials under same or comparable input blast loadings. In case of the plain composite materials, the "failure" point (deflections equaling 2.5 times the thickness) is produced at an earlier time compared to the layered system under comparable input blast loadings. Also, in case of the polyurea facing the blast, the failure point is not observed at all. The macroscopic damage in the plate also corroborate with the observed real time trend, vis-à-vis, the PU/EVE configuration showing lower damage area compared to the EVE/PU configuration.

Under the same input blast loadings, the sandwich configuration showed normalized deflections less than one, which is well within the elastic limits of the plate. Here again, it was observed that the PU/EVE configuration reached the failure point at a later time stage compared to the EVE/PU configuration. The delay in the attainment of this failure point between the layered configurations can

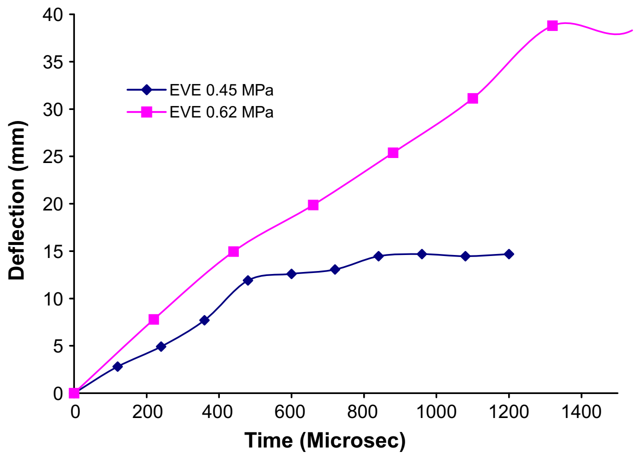

Fig. 21. Center point deflections of the plain composites (EVE) under different input blast pressures.

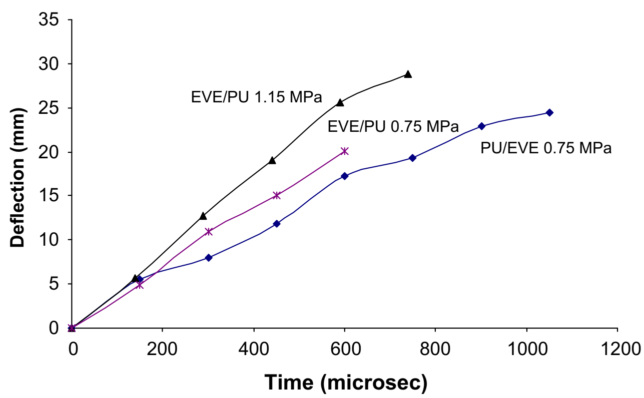

Fig. 22. Center point deflections of the layered materials under different input blast pressures.

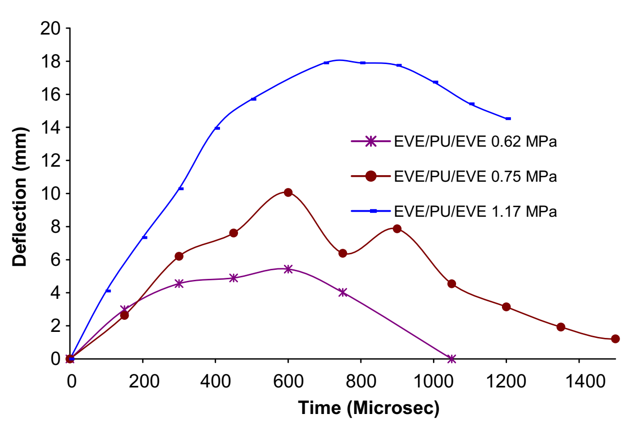

Fig. 23. Center point deflections of the sandwich materials under different input blast pressures.

be attributed to the internal strengthening mechanisms that are present in the PU/EVE system.

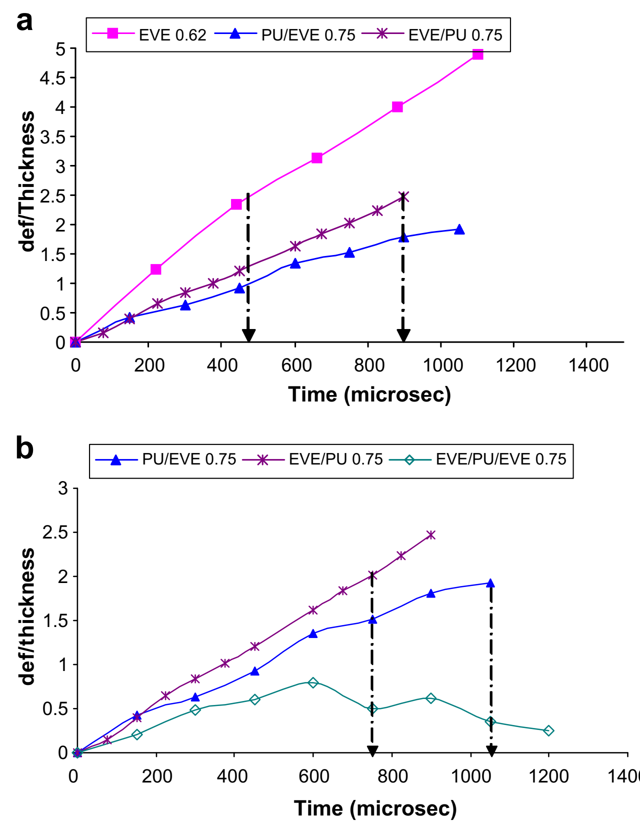

Fig. 24. Normalized center point deflections (per unit thickness) of (a) plain and layered composites and (b) layered and sandwich composite materials under comparable input blast.

5. Conclusions

The present study experimentally evaluated the blast resistance and damage behavior of plain–woven, layered and sandwich composites, fabricated using polyurea and glass fiber composite. A shock tube was utilized for applying the shock blast loading on simply supported rectangular plates of the above materials. The response of the plate was recorded real time using high-speed digital imaging. The plate deflections and damage behavior were observed in these high-speed images. Post impact damage was characterized using visual examination, microscopic study and a detailed post mortem analysis. It is observed that, layering of glass fiber composites with a soft layer provides better blast resistance. This enhancement of blast resistance is more pronounced when the soft material faces the blast. Above all, it is experimentally observed that, of the different possible material constructions, sandwich materials made of sandwiching a soft layer (PU) in between woven composite skins (EVE) had the best blast resistant properties. Simultaneously, the weight addition for the layered and sandwich composites are 60% more than the plain composite alone. But the performance enhancement in the layered material is about 25% better (when polyurea faces the blast) and in case of sandwich composite (EVE/

PU/EVE), the blast performance is enhanced by more than 100%.

Acknowledgement

The authors acknowledge the financial support and encouragement provided by Dr. Yapa Rajapakse, Office of Naval Research Grant Nos. N00014-04-1-0268 and N00014-01-1-1033.

References

[1] Wiezerbicki T, Nurick GN. Large deformation of thin plates under localized impulsive loading. Int. J Impact Eng 1996;18(7-8):899–918.
[2] Zhu L. Transient deformation modes of square plates subjected to explosive loadings. Int J Solids Struct 1996;33(3):301–14.
[3] Fleck NA, Deshpande VS. The resistance of clamped sandwich beams to shock loading. J Appl Mech 2004;71(3):386–401.
[4] Nurick GN, Gelman ME, Marshall NS. Tearing of blast loaded plates with clamped boundary conditions. Int J Impact Eng 1996;18(7-8):803–27.
[5] Galiev U. Experimental observations and discussion of counterintuitive behavior of plates and shallow shells subjected to blast loading. Int J Impact Eng 1996;18(7-8):783–802.
[6] Hammond L, Grzebieta R. Structural response of submerged air-backed plates by experimental and numerical analyses. Shock Vib 2000;7(6):333–41.
[7] Teng TL, Liang CC, Liao CC. Nonlinear forced vibration analysis of the rectangular plates by the Fourier series method. Comput Mech 1999;23(1):1–7.
[8] Ramajeyathilagam K, Vendhan CP. Deformation and rupture of thin rectangular plates subjected to underwater shock. Int J Impact Eng 2004;30(6):699–719.
[9] Fatt MS Hoo, Ouyang X, Dinan RJ. Blast response of walls retrofitted with elastomer coatings. Struct Mater 2004;15:129–38.
[10] Yi J, Boyce MC, Lee GF, Balizer E. Large deformation rate-dependent stress–strain behavior of polyurea and polyurethanes. Polymer 2006;47(1):319–29.
[11] Amirkhizi AV, Isaacs J, McGee J, Nemat-Nasser S. An experimentally-based viscoelastic constitutive model for polyurea, including pressure and temperature effects. Philos Mag 2006;86(36):5847–66.
[12] Roland CM, Twigg JN, Vu Y, Mott PH. High strain rate mechanical behavior of polyurea. Polymer 2007;48(2):574–8.
[13] Tekalur SA, Shivkumar K, Shukla A. Mechanical behavior and damage evolution in E-glass vinyl ester and carbon composites subjected to static and blast loads. Composites Part B: Engineering, in press. Available online 6 March 2007.
[14] Tekalur SA, Arun Shukla A, Ruggiero P. Blast loaded thin composite plates – an experimental study. In: 2006 SEM annual conference, St. Louis, June 2006.
[15] Swaminathan G, Shivakumar KN, Sharpe M. Mechanical properties of glass and T700 carbon vinyl ester composites. J Adv Mater 2006;38(2):52–63.
[16] Smith S, Emmanwori L, Sadler R, Shivakumar K. Evaluation of composite sandwich panels fabricated using vacuum assisted resin transfer molding. In: SAMPE 2000, Long Beach, CA, 2000.
[17] Sadler R, Sharpe M, Swaminathan G, Shivakumar K. Mechanical properties of panels fabricated by the VARTM processed composites using different fibers and fabric architectures. 18th Annual technical conference of ASC, University of Florida, Gainesville, FL, 2003.
[18] Lindholm US. Some experiments with the split Hopkinson pressure bar. J Mech Phys Solids 1964;12(5):317–35.
[19] Chalivendra VB, Shukla A, Bose A, Parameswaran V. Processing and mechanical characterization of lightweight polyurethane composites. J Mater Sci 2003;38(8):1631–43.
[20] LeBlanc J, Shukla A, Rousseau C, Bogdanovich A. Shock loading of three-dimensional woven composite materials. Compos Struct 2007;79(3):344–55.